*Electrochimica Acta*, Vol. 37, No. 15, pp. 2707–2714, 1992
Printed in Great Britain.

0013–4686/92 $5.00 + 0.00


# THE ANODIC DISSOLUTION OF COPPER IN HYDROCHLORIC ACID SOLUTIONS

F. K. CRUNDWELL
Department of Chemical Engineering, University of the Witwatersrand, P.O. Wits, 2050, South Africa

(*Received* 7 *November* 1991; *in revised form* 8 *April* 1992)

**Abstract**—The electrodissolution of copper in hydrochloric acid solutions at the rotating ring-disk electrode was found to be controlled by both mass transfer and reaction in the apparent-Tafel region in HCl concentrations of between 0.1 and 1.0 M. The proposed mechanism describes the adsorption of $CuCl_{ads}$ on the corroding copper surface and the diffusion of $CuCl_2^-$ from the copper surface. The reaction in the limiting-current region was found to be controlled by the diffusion of $Cl^-$ to the copper surface through a porous CuCl layer that forms on the surface. The thickness of this porous layer is dependent on the stirring conditions, and independent of the $Cl^-$ concentration. $Cu^{2+}$ is also produced at the Cu surface during electrodissolution. A mechanism describing the formation of a porous film of CuCl on the surface, the diffusion of $Cl^-$ through this film and the formation of $Cu^{2+}$ has been proposed.

*Key words:* copper, dissolution, hydrochloric acid, corrosion, cuprous chloride.

## INTRODUCTION

Copper and its alloys are used extensively in marine environments because of their good resistance to seawater. For this reason, and because the electrodissolution of Cu in chloride solutions is important in electropolishing and electromachining, attention has been focussed on this reaction.

Typical steady-state polarization curves for the electrodissolution of Cu can be divided into three regions, (1) the apparent-Tafel region, associated with the formation of $CuCl_2^-$, is observed at relatively low current densities; (2) the limiting-current region, associated with the formation of a CuCl film, is observed at higher current densities; and (3) the region beyond the limiting-current plateau, in which the current density increases due to the formation of $Cu^{2+}$. Lee and Nobe[1] report the occurrence of a current peak between the apparent-Tafel and limiting-current regions during potential sweep experiments.

The electrodissolution of copper in the apparent-Tafel region has been found to follow Tafel-like behaviour, with a slope of 60 mV/decade, and has been found to be strongly dependent on stirring conditions, suggesting that the reaction is controlled by both mass-transfer and activation processes[1–9]. At chloride concentrations of less than 1 M the rate of reaction is proportional to $[Cl^-]^2$, reflecting the formation of $CuCl_2^-$, while at higher concentrations the reaction is proportional to $[Cl^-]^x$ where $x > 2$.

Several mechanisms involving both reaction and mass transfer of $CuCl_2^-$ from the electrode surface to the bulk solution have been proposed to describe the kinetics of dissolution in the apparent-Tafel region[1, 3, 7, 10].

At higher anodic potentials, a porous film of CuCl forms on the surface, and the current reaches its limiting value. This limiting-current density has been found to be strongly dependent on the stirring conditions, and is proportional to the concentration of the chloride ion[1–9]. These observations suggest that the reaction is mass transfer controlled in this potential region, and several mechanisms involving the convective diffusion of $Cl^-$ through the boundary layer or the diffusion of $Cl^-$ through the porous film have been proposed[1, 5].

Most investigators who have studied this reaction have used steady-state techniques and have focused on the kinetics of dissolution in the apparent-Tafel region. The purpose of this study is to analyse the anodic reaction including the limiting-current region using both steady-state and *ac*-impedance techniques. In this paper we report the results of the steady-state measurements using a rotating ring-disk electrode, and provide an analysis of the reaction that is consistent with the results of the *ac*-impedance investigation. These impedance results are presented and analysed in a subsequent paper. The contribution that this paper intends to make is to provide a simple and consistent interpretation of the steady-state results reported here. This interpretation of the steady-state results provides a model which succesfully describes the *ac*-impedance results.

## EXPERIMENTAL

A rotating ring-disk electrode assembly was used for all the potential-sweep and steady-state measurements. The electrode consisted of a copper disk with a diameter of 0.35 cm and a platinum ring. The ring had an internal diameter of 0.45 cm and an external diameter of 0.6 cm. The electrode was constructed so that a gap between the ring and the disk was filled with Araldite epoxy, and these two electrodes were inserted in a teflon holder. The counter electrodes

were made of platinum. A saturated calomel electrode was used as the reference, and all potentials were referred to this electrode. The collection efficiency of the ring was determined to be 0.37. This is in good agreement with the theoretical collection efficiency, which was calculated by the method of Albery and Bruckenstein[11] to be 0.3859. The electrode was polished with 1200 grit waterpaper and less than 5 $\mu$m alumina paste prior to each experiment.

Analytical grade hydrochloric acid and deionized water were used. All experiments were at 25°C.
were manufactured at MINTEK, and the currents and potentials were recorded on an HP 7090A measurement system. The ring potential was set to +610 mV vs. *sce* to detect cuprous ions by oxidizing them to cupric ions, and set to −100 mV vs. *sce* to detect cupric ions in the limiting-current region by reducing them to cuprous ions. The current at the ring with the ring potential set at −100 mV vs. *sce* was found to be less than 5 $\mu$A.

The methods of linear sweep voltammetry and steady-state polarization were used in this study. The rate at the disk was maintained at 0.18 mV/s. Steady-state measurements were made once the current had stabilized for a few minutes.

## RESULTS

Results of the linear potential-sweep investigation of the anodic dissolution of Cu from a rotating disk for solutions of different hydrochloric acid concentrations indicate an apparent-Tafel region with a slope of 70 mV/decade at low overpotentials, and a limiting-current region at high overpotentials. The anodic dissolution of Cu is known to exhibit a strong dependence on the stirring conditions. Results for different rotation speed on the electrodissolution of Cu indicate that the current is dependent on the rotation speed in both the apparent-Tafel region, and the limiting-current region.

These results indicate that the mechanism of dissolution in the apparent-Tafel region is controlled by both the reaction kinetics and by diffusion. Mixed kinetics such as these are normally analysed by plotting $1/i_D$ against $1/\omega^{1/2}$, where $i_D$ is the disk current, and $\omega$ is the rotation speed. The intercept of this plot represents the kinetics of the reaction as $\omega \to \infty$, that is, when the mass transfer effects are negligible, while the slope is dependent on both mass transfer and kinetic factors.

Results of the steady-state investigation, plotted in this form, are presented in Fig. 1, illustrating the effect of the concentration of $Cl^-$ on the anodic current density. The electrodissolution of Cu is known to be independent of the pH, but Fig. 1 emphasizes the strong dependence this reaction has on the $Cl^-$ concentration. The $Cl^-$ concentration was limited to less than 1 M, where the reaction is known to be second order with respect to $Cl^-$[1]. At higher $Cl^-$ concentrations the rate has been reported to be higher than 2[5], due to the formation of $CuCl_3^{2-}$ and higher $Cl^-$ complexes.

The dependence of the inverse of the intercept, $i_\infty$, and the slope, $\partial i_D^{-1}/\partial\omega^{-1/2}$, on the $Cl^-$ concentration are shown in Figure 2 as log–log plots. Figure 2 indicates that $i_\infty$ is proportional to $[Cl^-]^{1.38}$ and the slope, $\partial i_D^{-1}/\partial\omega^{-1/2}$, is proportional to $[Cl^-]^{-1.92}$.

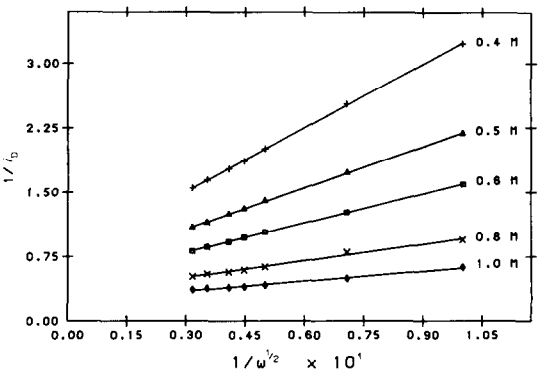


Fig. 1. A plot of $1/i$ against $1/\omega^{1/2}$ for a copper rotating-disk in solutions with different concentrations of HCl at −100 mV.

The effect of the rotation speed on the current density at constant potential is shown in Fig. 3. The dependence of the inverse of the intercept, $i_\infty$, and the slope, $\partial i_D^{-1}/\partial\omega^{-1/2}$, on the potential is shown in Fig. 4. $i_\infty$ has a dependence of 90 mV/decade on the potential while $\partial i_D^{-1}/\partial\omega^{-1/2}$ has a dependence of −69 mV/decade.

Previous experimental results are presented in Table 1. The table clearly illustrates the gaps in the

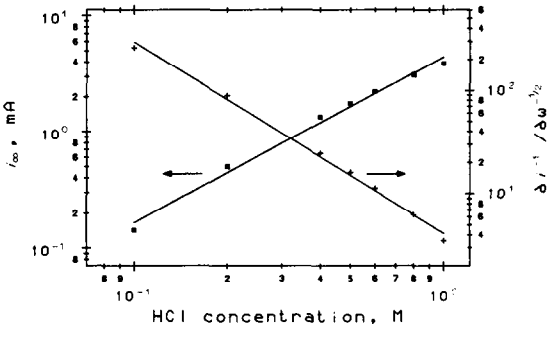


Fig. 2. The effect of the HCl concentration on the slope and the inverse of the intercept ($i_\infty$) of the plots in Fig. 1.

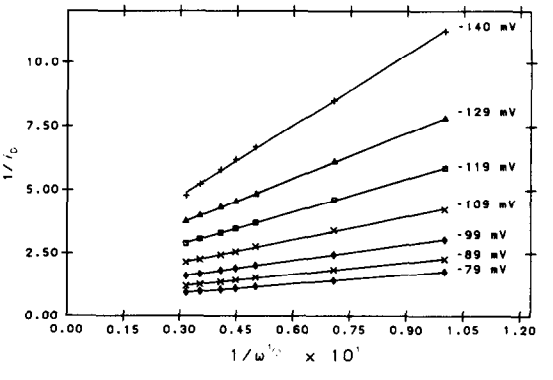


Fig. 3. A plot of $1/i$ against $1/\omega^{1/2}$ for different potentials in 0.5 M HCl.

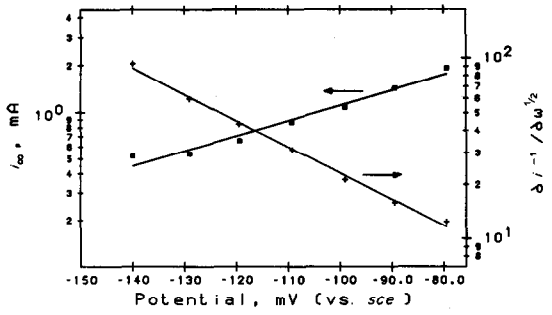


Fig. 4. The effect of potential on the slope and the inverse of the intercept ($i_\infty$) of the plots in Fig. 3.

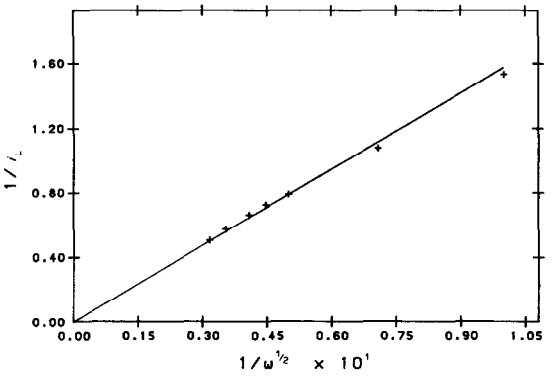


Fig. 6. A plot of $1/i_L$ against $1/\omega^{1/2}$ at 20 mV in 0.5 M HCl.

analysis of previous experimental work. The intercept, $i_\infty$, has not been examined in detail, particularly with respect to its dependence on the concentration of $Cl^-$. The results presented here are in agreement with previously reported work, particularly with respect to the work of Lee and Nobe[1] and Walton and Brook[12].

The results for the steady-state measurements in the limiting-current region are shown in Figs 5 and 6. Figure 5 indicates that the limiting-current density is proportional to $[Cl^-]$, while Fig. 6 indicates that the dissolution of Cu in the limiting-current region is governed by mass transport effects.

Figure 7 is a plot of $1/i_R$, the inverse of the ring current at 610 mV, against $1/\omega^{1/2}$, and these results do pass through the origin. Since the ring current is proportional to the flux of $CuCl_2^-$, this indicates that the flux of $CuCl_2^-$ is governed by mass transfer only.

Experiments, similar to those conducted by Lee *et al.*[8], were performed to obtain a measure of the relative thickness of the CuCl film. The disk potential was set at a fixed potential for 10 min to allow the film to grow and reach a steady thickness, and the ring potential was set at 610 mV to record the rate of formation of the cuprous species. When the disk current is switched off, the dissolution of the film is detected at the ring, and the areas under the ring current–time curve is a measure of the relative film thickness at the time the disk current was switched off.

These results indicated that there is essentially no film formation in the apparent-Tafel region, while there is a substantial film in the limiting-current region. Integration of these current-time curves gives a relative measure of the film thickness, assuming that the porosity is constant in all the experiments. The relative film thickness, expressed as the integral of the ring current–time curve measured in mA, is plotted in Figs 8 and 9. Figure 8 indicates that the

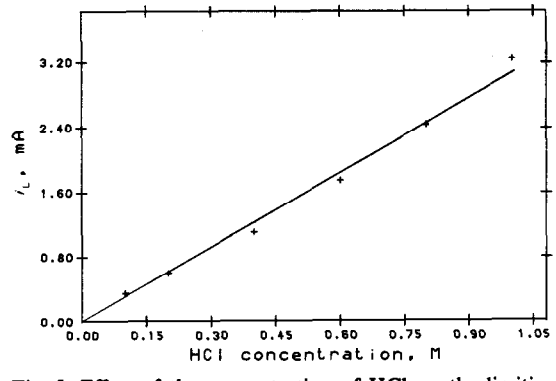


Fig. 5. Effect of the concentration of HCl on the limiting current of a rotating copper disk at 500 rpm, $V_D = 20$ mV.

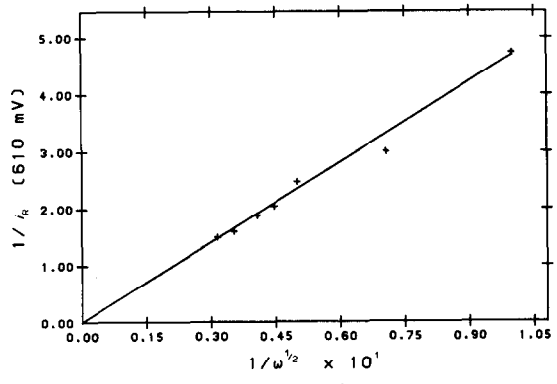


Fig. 7. A plot of $1/i_R$ against $1/\omega^{1/2}$ at a ring potential of 610 mV. Disk potential at 20 mV. 0.5 M HCl.

Table 1. Comparison of experimental results for the dissolution of Cu in the apparent-Tafel region

| Source | $\left(\frac{\partial \log i_\infty}{\partial E}\right)_{[Cl^-]}$ mV/dec | $\left(\frac{\partial \log i_\infty}{\partial \log[Cl^-]}\right)_E$ | $\left(\frac{\partial \log \Upsilon}{\partial E}\right)_{[Cl^-]}$ mV/dec | $\left(\frac{\partial \log \Upsilon}{\partial \log[Cl^-]}\right)_E$ |
|---|---|---|---|---|
| Moreau *et al.*[7] | 0* | 0* | −60 | −2.0 |
| Lee and Nobe[1] | ND | ND | −60 | −1.8 |
| Smyrl[3] | 120 | ND | −60 | ND |
| Walton and Brook[12] | 84 | ND | −63 | ND |
| Present study | 90 | 1.38 | −69 | −1.92 |

$\Upsilon$ is the slope of the plot of $1/i_D$ vs. $1/\omega^{1/2}$, *ie* $\Upsilon = \partial i_D^{-1}/\partial\omega^{-1/2}$.
* Moreau *et al.*[7] reported that $i_\infty = 0$.
ND = not determined or not reported.

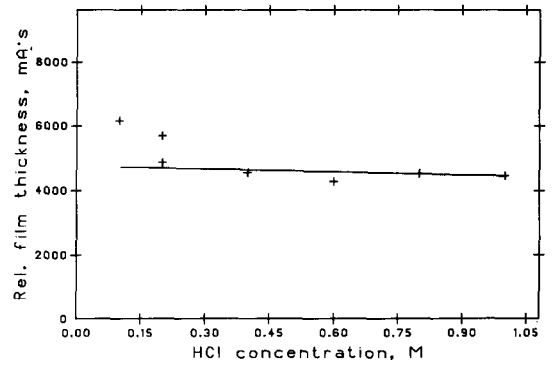


Fig. 8. The effect of the HCl concentration on the relative film thickness of the CuCl porous layer at a disk potential of 20 mV and at 500 rpm.

relative film thickness is independent of the $Cl^-$ concentration although there is some scatter in the data, and Fig. 9 indicates that it is dependent on the rotation speed, with an order of dependence of $-0.46$. This is close to the half-order dependence expected if convective diffusion is the controlling mechanism.

$Cu^{2+}$ is formed at the disk at higher anodic potentials. The formation of $Cu^{2+}$, detected at the ring with the ring potential set to $-100$ mV, is dependent on the rotation speed, as shown in Fig. 10. It is important to point out that this dependence is the opposite of that expected if the rate of formation of $Cu^{2+}$ is controlled by convective mass transfer.

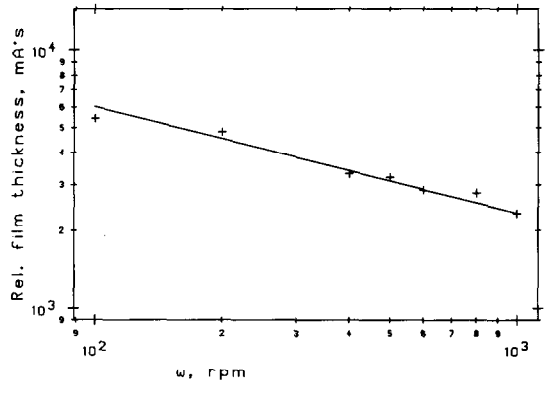


Fig. 9. The effect of the rotation speed on the relative film thickness of the CuCl porous layer at a disk potential of 20 mV in 0.5 M HCl.

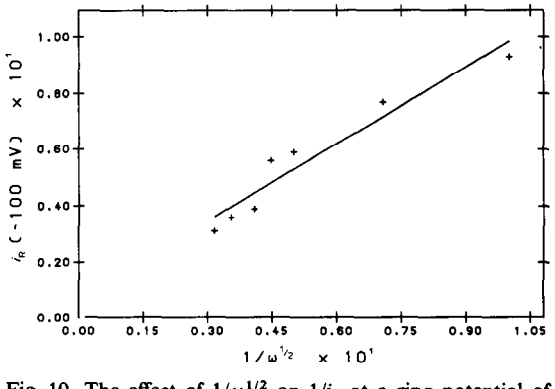


Fig. 10. The effect of $1/\omega^{1/2}$ on $1/i_R$ at a ring potential of $-100$ mV (set to detect $Cu^{2+}$ ions) at a disk potential of 100 mV in 0.5 M HCl.

## DISCUSSION

*Apparent-Tafel region*

In the apparent-Tafel region, no cuprous chloride film has been reported to form on the electrode surface and $CuCl_2^-$ has been shown to be the limiting diffusion species[1–3]. In addition, no formation of $Cu^{2+}$ in the apparent-Tafel region has been reported[1–9].

The electrodissolution of Cu in $Cl^-$ solutions (less than 1 M) may be expressed in terms of the following mechanism. The initial step is the electroadsorption of $Cl^-$ by the reaction:

$$Cu + Cl^- \underset{k_{-1}}{\overset{k_1}{\rightleftharpoons}} CuCl_{ads} + e^-. \quad (1)$$

$CuCl_{ads}$ represents a cuprous chloride species which is adsorbed onto the copper electrode surface.

The rate of the electrochemical reaction[1] is given by

$$\frac{i_1}{F} = k_1 C_2(0)(1-\theta) - k_{-1}\theta \quad (2)$$

where $\theta$ is the surface coverage of the $CuCl_{ads}$ adsorbed intermediate, and $C_2(0)$ is the concentration of $Cl^-$ at the Cu surface. The electrochemical rate constants $k_1$ and $k_{-1}$ are dependent on the potential. The first term on the right-hand side represents the anodic term, while the second term is the cathodic term.

Reaction[1] may be followed by the formation of soluble cuprous chloride by the reaction:

$$CuCl_{ads} + Cl^- \underset{k_{-2}}{\overset{k_2}{\rightleftharpoons}} CuCl_2^-. \quad (3)$$

The rate of formation of $CuCl_{ads}$ is governed by the material balance equation

$$\frac{d\theta}{dt} = \frac{i_1}{F} - k_2 C_2(0)\theta + k_{-2} C_1(0). \quad (4)$$

The terms on the right-hand side of the above equation represent the net production of $CuCl_{ads}$ by reactions[1], and [2]. $C_1(0)$ is the concentration of $CuCl_2^-$ in solution at the electrode surface.

A simplified model of the transport processes occurring during the dissolution in the apparent-Tafel region is shown in Fig. 11b. The concentration gradient of $CuCl_2^-$ is determined by convective diffusion

$$\frac{\partial C_1}{\partial t} = D_1 \frac{\partial^2 C_1}{\partial x^2} - v_x \frac{\partial C_1}{\partial x} \quad x > 0. \quad (5)$$

The origin of the $x$-coordinate is taken at the Cu-solution interface. This differential equation is

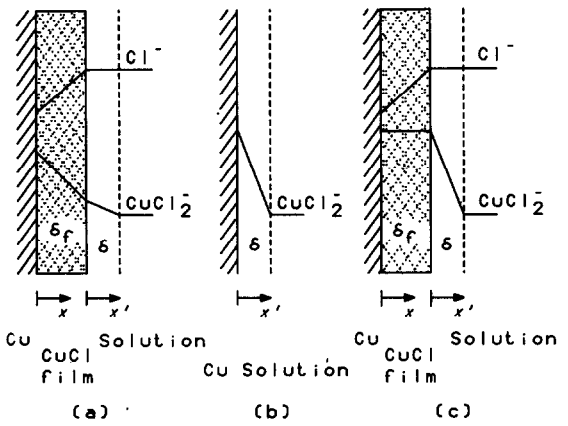


Fig. 11. Schematic diagram to illustrate the various diffusion processes that may be occurring during the dissolution of copper (a). Also illustrated are the proposed models for the apparent-Tafel region (b) and for the limiting-current region (c).

subject to the following boundary conditions:

$$x = 0 \qquad N_1(0) = k_2\,\theta C_2(0) - k_{-2}\,C_1(0). \tag{6}$$

$$x = \infty \qquad C_1(\infty) = 0. \tag{7}$$

If it is assumed that $\theta$ is sufficiently small so that $1 - \theta \approx 1$, and that there is no concentration gradient of $Cl^-$ so that $C_2(0) = C_2$, where $C_2$ is the bulk concentration of $Cl^-$, then Equation (2) becomes

$$\frac{i_1}{F} = k_1 C_2 - k_{-1}\theta. \tag{8}$$

The $CuCl_2^-$ concentration gradient is given by Equation (5) and the boundary conditions, Equations (6) and (7). Solving Equation (5) and Equation (4) for $\theta$ at steady-state and substituting these expressions into Equation (8) gives

$$\frac{F}{i} = \frac{1}{k_1 C_2} + \frac{k_{-1}}{k_1 k_2 C_2^2} + \frac{k_{-1}k_{-2}}{k_1 k_2 C_2^2}\frac{\delta}{D_1'} \tag{9}$$

where $\delta = 1.805 D_1'^{1/3}\nu^{1/6}\omega^{-1/2}$ is the steady-state diffusion layer thickness on the rotating-disk electrode, and which is related to the Nernst stagnant diffusion layer thickness by $\delta_N = 0.89298\ \delta$. Since $k_1 = k_1' \exp\{-(1-\alpha)FE/RT\}$, Equation (9) may be rewritten as

$$\frac{F}{i} = \frac{1}{k_1' C_2 \exp\{\alpha FE/RT\}} + \frac{k_{-1}'}{k_1' k_2 C_2^2 \exp\{FE/RT\}} + \frac{k_{-1}' k_{-2}\tau\omega^{-1/2}}{k_1' k_2 C_2^2 \exp\{FE/RT\}} \tag{10}$$

where $\tau = 1.805 D_1'^{-2/3}\nu^{1/6}$, and $\nu$ is the viscosity.

Figures 1 to 4 indicate that Equation (10) does account for the features of this reaction. Figures 2 and 4 show that the slope, $\partial i_D^{-1}/\partial\omega^{-1/2}$, is proportional to $[Cl^-]^{-1.92}$ and has a potential dependence of $-69$ mV/decade. Both these results are close to those predicted by Equation (10), *ie* proportional to $[Cl^-]^{-2}$ and a potential dependence of $-60$ mV/decade. Figures 2 and 4 show that the inverse of the intercept, $i_\infty$, is proportional to $[Cl^-]^{1.38}$, and has a potential dependence of 90 mV/decade. Equation (10) predicts that $i_\infty$ should be proportional to $[Cl^-]^x$ where $x$ is between 1 and 2, and should have a potential dependence of between 60 and 120 mV/decade. Therefore, Equation (10) successfully describes the kinetics of dissolution of copper in the apparent-Tafel region.

Previous models for the dissolution of copper in the apparent-Tafel region may be compared by examining the dependence of the inverse of the intercept, $i_\infty$, and the slope, $\partial i_D^{-1}/\partial\omega^{-1/2}$, on potential and chloride concentration.

Table 2 summarizes the model results of previous work. The models of Smyrl[3], Lee and Nobe[1], Moreau[6 and 7] and Tribollet and Newman[10] all suggest that the slope has a dependence of 60 mV/decade on the potential and is proportional to $[Cl^-]^2$. This is in good agreement with the results presented in Figs 1 to 4.

The models of Lee and Nobe[1], and Tribollett and Newman[10] suggest that $i_\infty$ is proportional to $[Cl^-]^2$, while the model of Smyrl[3] suggests that $i_\infty$ is independent of $[Cl^-]$. These models are clearly not in agreement with the experimental results which are proportional to $[Cl^-]^{1.38}$. Similarly, the models of Smyrl[3] and Tribollet and Newman[10] suggest that $i_\infty$ has a dependence of 120 mV/decade on the potential while the model of Lee and Nobe[1] has a potential dependence of 60 mV/decade. Again these models are not in agreement with the experimental results which have a dependence of 90 mV/decade on the potential. Therefore, it is concluded that equation (10) is a more successful description of the reaction mechanism than previously published models.

Table 2. Comparison of model results for the dissolution of Cu in the apparent-Tafel region

| Source | $\left(\frac{\partial \log i_\infty}{\partial E}\right)_{[Cl^-]}$ mV/dec | $\left(\frac{\partial \log i_\infty}{\partial \log[Cl^-]}\right)_E$ | $\left(\frac{\partial \log \Upsilon}{\partial E}\right)_{[Cl^-]}$ mV/dec | $\left(\frac{\partial \log \Upsilon}{\partial \log[Cl^-]}\right)_E$ |
|---|---|---|---|---|
| Moreau *et al.*[7] | 0 | 0 | −60 | −2 |
| Lee and Nobe[1] | 60 | 2 | −60 | −2 |
| Tribollett and Newman[10] | 120 | 2 | −60 | −2 |
| Smyrl[3] | 120 | independent | −60 | −2 |
| Present model | 60 to 120 | 1 to 2 | −60 | −2 |
| Present study | 90 | 1.38 | −69 | −1.92 |

$\Upsilon$ is the slope of the plot of $1/i_D$ vs. $1/\omega^{1/2}$, *ie* $\Upsilon = \partial i_D^{-1}/\partial\omega^{-1/2}$.

*Limiting-current region*

A limiting-current region has been reported at higher current densities. This limiting-current plateau is associated with the precipitation of a porous CuCl layer on the copper surface. Previous researchers[1, 2, 8, 9] have agreed that the reaction in the limiting-current region is controlled by the transport of $Cl^-$ to the reacting surface. This means that there is a change in the controlling mechanism as the potential moves from the apparent-Tafel region to the limiting-current region, since the transport limitation in the apparent-Tafel region was the transport of $CuCl_2^-$ ions from the reacting surface. This suggests film formation is due to a mechanism where the rate of diffusion of $Cl^-$ cannot match the rate of production of $CuCl_2^-$. The product of the reaction under these conditions is aqueous CuCl, and since the solubility of CuCl is low, crystalline CuCl precipitates at the surface of the electrode, and this initiates the growth of a porous film.

This process can be represented by the initial formation of the adsorbed cuprous chloride species:

$$Cu + Cl^- \xrightarrow{k_1} CuCl_{ads} + e^-. \qquad (11)$$

It is assumed that at these potentials reaction equation (11) will proceed in the forward direction only, so that equation (2) becomes

$$\frac{i_1}{F} = k_1(1 - \theta)C_2(0). \qquad (12)$$

Reaction (11) is followed by the precipitation of a CuCl film on the surface of the electrode by the reaction:

$$CuCl_{ads} \xrightarrow{k_3} CuCl_{(film)}. \qquad (13)$$

It may be that the adsorbed species $CuCl_{ads}$ may not be the direct precursor to the precipitation of crystalline CuCl but rather that it forms from the precipitation of aqueous CuCl. However, the analysis following is the same whether we refer to this species as aqueous CuCl [provided the product of reaction (11) is aqueous CuCl which precipitates in the vicinity of the electrode–salt interface] or as adsorbed $CuCl_{ads}$.

It is assumed that the crystalline CuCl that precipitates on the surface of the electrode is not electrically conductive; therefore, the electrochemical reaction can only take place on the bare copper surface.

The porous film may dissolve chemically by the reaction:

$$CuCl_{(film)} + Cl^- \underset{k_{-4}}{\overset{k_4}{\rightleftharpoons}} CuCl_2^-. \qquad (14)$$

$Cu^{2+}$ has been detected in the limiting-current region, and may form by a mechanism such as:

$$CuCl_{ads} \underset{k_{-5}}{\overset{k_5}{\rightleftharpoons}} Cu^+_{ads} + Cl^- \qquad (15)$$

$$Cu^+_{ads} \xrightarrow{k_6} Cu^{2+} + e^-. \qquad (16)$$

The rate of the electrochemical reaction (16) is given by

$$\frac{i_2}{F} = k_6\Gamma \qquad (17)$$

where $\Gamma$ is the surface coverage of the $Cu^+_{ads}$ adsorbed intermediate. In writing the rate in this form it is assumed that the reverse reaction is negligible, that is, the cathodic term is negligible.

The rate of formation of $CuCl_{ads}$ is governed by the material balance:

$$\frac{d\theta}{dt} = \frac{i_1}{F} - k_3\theta - k_5\theta + k_{-5}\Gamma C_2(0). \qquad (18)$$

The terms on the right-hand side of the above equation represent the net production of $CuCl_{ads}$ by reactions (11), (13) and (15). The formation and dissolution of the porous film is given by material balance:

$$\rho_{CuCl}(1 - \varepsilon)\frac{d\delta_f}{dt} = k_3\theta - k_4 C_b + k_{-4}C_1'(0) \qquad (19)$$

where $\varepsilon$ is the voidage of the porous film, $\rho_{CuCl}$ is the molar density of crystalline CuCl. The first term on the right-hand side of the equation represents the growth of the film at the electrode–film interface while the second and third terms represent the dissolution of the film at the film–solution interface.

A material balance for the $Cu^+_{ads}$ intermediate gives

$$\frac{d\Gamma}{dt} = k_5\theta - k_{-5}\Gamma C_2 - k_6\Gamma. \qquad (20)$$

The first two terms on the right-hand side of this equation represent the net production of $Cu^+_{ads}$ by reaction (15) and the third term represents the consumption of $Cu^+_{ads}$ by reaction (16).

A simple model for the dissolution of Cu in the limiting-current region is that illustrated in Fig. 1c. If $CuCl_2^-$ is saturated within the CuCl porous film, so that the flux of $CuCl_2^-$ within the film is zero, *ie* $N_1(\delta_f) = 0$. This then implies that all the $CuCl_2^-$ that is detected at the ring is formed by the reaction with the film at the film–solution interface.

The concentration gradient of $Cl^-$ in the porous layer is determined by molecular diffusion

$$\frac{\partial C_2}{\partial t} = D_2\frac{\partial^2 C_2}{\partial x^2} \quad 0 > x > \delta_f. \qquad (21)$$

The origin of the $x$-coordinate is taken at the $Cu–CuCl_{(film)}$ interface. The differential equation (21) is subject to the following boundary conditions:

$$x = 0 \qquad N_2(0) = \frac{i_1}{F} - k_5\theta + k_{-5}\Gamma C_2(0) \qquad (22)$$

$$x = \delta_f \qquad C_2(\delta_f) = C_2 \qquad (23)$$

$N$ represents the flux, $\delta_f$ is the film thickness, and $C_2$ is the bulk concentration of $Cl^-$.

The concentration gradient of $CuCl_2^-$ is determined by convective diffusion

$$\frac{\partial C_1'}{\partial t} = D_1'\frac{\partial^2 C_1'}{\partial x'^2} - v_{x'}\frac{\partial C_1'}{\partial x'} \quad x' > 0. \qquad (24)$$

The origin of the $x'$-coordinate is taken at the $CuCl_{(film)}$-solution interface, *ie* $x' = x - \delta_f$. $C'_1$ is the concentration of $CuCl_2^-$ in the solution, and $D'_1$ is the diffusion coefficient of $CuCl_2^-$.

$$x' = 0 \qquad N'_1(0) = k_4 C_2(\delta_f) - k_{-4} C'_1(0) \tag{25}$$

$$x' = \infty \qquad C'_1(\infty) = 0. \tag{26}$$

This model has neglected all effects, such as field-assisted migration, that are not described by convective or molecular diffusion. It has also assumed that the molecular diffusion within the porous layer is described by a single effective diffusion coefficient, that the porosity of the CuCl film is uniform, that there are no variations other than those in the $x$-direction, and that the interfaces are planar and perpendicular to the axis of rotation.

It is assumed that there is no accumulation of dissolved material in the porous salt layer, and that the concentration profiles are established instantaneously. This is the pseudo-steady state assumption. The application of this assumption contradicts the suggestion of Pearlstein *et al.*[9] that the current oscillations sometimes found in Cu electrodissolution are due to the non-linearity introduced into these equations by the moving-boundary conditions. Rather, the non-linearities are due to the actual reaction mechanism

Since little $CuCl_2^-$ is formed at the electrode surface in the limiting-current region, the concentration of the $CuCl_{ads}$ intermediate is given by:

$$\theta = \frac{k_1 C_2(0) + k_{-5}\Gamma C_2(0)}{k_1 C_2(0) + k_3 + k_5}. \tag{27}$$

If we assume that $k_6$ is small, then $\Gamma$ is given by

$$\Gamma = \frac{k_5 \theta}{k_{-5} C_2(0)}. \tag{28}$$

Integrating Equation (21), applying the boundary conditions Equations (22) and (23), and substituting Equations (27) and (28) for $\theta$ and $\Gamma$ gives an expression for the steady-state value of $C_2(0)$ that is quadratic. If we neglect terms in $C_2(0)^2$, the steady-state value of $C_2(0)$ is given by

$$C_2(0) = \frac{C_2/k_1}{1/k_1 + \delta_f/D_2 - C_2/k_3}. \tag{29}$$

Substituting Equations (27)–(29) into Equation (12), and simplifying, we get

$$\frac{i_1}{F} = \frac{C_2}{1/k_1 + \delta_f/D_2}. \tag{30}$$

Since we have assumed that no $CuCl_2^-$ is formed at the Cu surface, $k_4 C_2 - k_{-4} C'_1(0)$ is the flux of $CuCl_2^-$ from the disk, and this flux is detected as the ring current when the ring potential is set to 610 mV. If we solve Equation (24) and substitute the boundary conditions, Equations (25) and (26), we get an expression for the flux of $CuCl_2^-$ from the disk.

$$N'_1(0) = \frac{k_4 C_2 D'_1/\delta}{D'_1/\delta + k_{-4}}. \tag{31}$$

If we assume that $k_{-4} \gg D'_1/\delta$, then a plot of $F/i_R$ against $\omega^{-1/2}$ will pass through the origin. Figure 7 indicates that this assumption is valid.
Thus, Equation (19) becomes

$$0 = \frac{k_3 k_1 C_2(0)}{k_1 C_2(0) + k_3} - \frac{D'_1}{\delta}\frac{k_4 C_b}{k_{-4}}. \tag{32}$$

Substituting Equations (27) and (28) into Equation (32) and solving this for $\delta_f$ gives

$$\frac{\delta_f}{D_2} = \frac{\delta}{D'_1}\frac{k_{-4}}{k_4} - \frac{1}{k_1}. \tag{33}$$

Equation (33) indicates that the film thickness should be independent of the $Cl^-$ concentration and should be proportional to $\omega^{-1/2}$. This is in good agreement with the experimental results shown in Figs 8 and 9.

Substituting Equation (33) into Equation (30) gives an expression for the limiting-current density in terms of the observed variables

$$\frac{i_1}{F} = \frac{D'_1 C_2 k_4}{k_{-4}} = \frac{C_2 k_4 \omega^{1/2}}{\tau k_{-4}}. \tag{34}$$

Figures 5 and 6 show that Equation (34) describes the dissolution kinetics in the limiting-current region.

$Cu^{2+}$ has been detected in the limiting-current region in this study and by others. The flux of $Cu^{2+}$ detected at the ring with the ring potential at $-100$ mV is proportional to $\omega^{-1/2}$, the inverse of that expected if the flux of $Cu^{2+}$ was dependent on convective diffusion. The contribution to the disk current due to this reaction is given by Equation (17). Combining Equation (17) with Equations (27)–(29) and (33) gives an expression for the current at the ring due to the formation of $Cu^{2+}$ in terms of the observed variables

$$\frac{i_2}{F} = \frac{k_6 k_5 k_1 \tau \omega^{-1/2}}{k_{-5} k_4 C_2}. \tag{35}$$

Equation (35) indicates that the plot of $i_R$ ($-100$ mV) vs. $1/\omega^{1/2}$ has a positive slope (Fig. 10). The line drawn through the data in Fig. 10 does not pass through the origin, while Equation (35) does. However, there is considerable uncertainty in the data represented in that figure. The reaction to form $Cu^{2+}$ has not been studied in detail in this work, and it is recommended that further study in the limiting-current region focuses on this reaction.

## CONCLUSIONS

The steady-state electrodissolution of Cu in HCl solutions has been studied, and mechanisms for the dissolution in the apparent-Tafel and limiting-current regions have been developed. This work has shown that the electrodissolution of Cu is described by a mechanism in which $CuCl_{ads}$ is formed on the surface as an intermediate species. In the apparent-Tafel region this intermediate reacts with $Cl^-$ ions to form $CuCl_2^-$, and both the reaction and the rate of mass transfer of $CuCl_2^-$ from the electrode surface are rate controlling. In the limiting-current region, the $CuCl_{ads}$ intermediate reacts to form a surface

layer of crystalline, porous CuCl on the surface, and the rate of mass transfer of $Cl^-$ through this porous layer is rate-determining.

## REFERENCES


1. H. P. Lee and K. Nobe, *J. electrochem. Soc.* **133,** 2035 (1986).
2. M. Braun and K. Nobe, *J. electrochem. Soc.* **126,** 1666 (1979).
3. W. H. Smyrl, *J. electrochem. Soc.* **132,** 1555–1562 (1985).
4. R. S. Cooper and J. H. Bartlett, *J. electrochem. Soc.* **105,** 109 (1958).
5. C. H. Bonfiglio, H. C. Albaya and O. A. Cobo, *Corrosion Sci.* **13,** 717 (1973).
6. A. Moreau, *Electrochim. Acta* **26,** 497 (1981).
7. A. Moreau, J. P. Frayret, F. Delrey and R. Pointeau, *Electrochim. Acta* **27,** 1281 (1982).
8. H. P. Lee, K. Nobe and A. Pearlstein, *J. electrochem. Soc.* **132,** 1031 (1985).
9. A. Pearlstein, H. P. Lee and K. Nobe, *J. electrochem. Soc.* **132,** 2159 (1985).
10. B. Tribollet and J. Newman, *J. electrochem. Soc.* **131,** 2780 (1984).
11. S. Bruckenstein and W. J. Albery, *Trans. Faraday Soc.* **62,** 1920 (1966).
12. M. E. Walton and P. A. Brook, *Corrosion Sci.* **17,** 317 (1977).